



HAL
open science

Microstructure evolution of ceramics during sintering : an analysis based on local image analysis measurements in the vicinity of controlled defects

E Girard, J M Chaix, C Carry, F Valdivieso, P Goeuriot, J L chelle

► To cite this version:

E Girard, J M Chaix, C Carry, F Valdivieso, P Goeuriot, et al.. Microstructure evolution of ceramics during sintering : an analysis based on local image analysis measurements in the vicinity of controlled defects. Sintering'05 : 4th international conference on science, technology and applications of sintering, Aug 2005, Grenoble,france, France. hal-03362787

HAL Id: hal-03362787

<https://hal.science/hal-03362787v1>

Submitted on 2 Oct 2021

HAL is a multi-disciplinary open access archive for the deposit and dissemination of scientific research documents, whether they are published or not. The documents may come from teaching and research institutions in France or abroad, or from public or private research centers.

L'archive ouverte pluridisciplinaire **HAL**, est destin e au d p t et   la diffusion de documents scientifiques de niveau recherche, publi s ou non,  manant des  tablissements d'enseignement et de recherche fran ais ou  trangers, des laboratoires publics ou priv s.

Microstructure evolution of ceramics during sintering : an analysis based on local image analysis measurements in the vicinity of controlled defects

E.Girard^{2,3}, J.M. Chaix¹, C.Carry¹, F.Valdivieso², P.Goeuriot², J.Léchelle³

¹Laboratoire de Thermodynamique et de Physico-Chimie Métallurgiques, INPGrenoble & CNRS UMR5614, BP 75, F-38402 Saint Martin d'Hères cedex, France; ²Dept. Céramiques Spéciales, ENSM Saint Etienne, France ;

²Ecole Nationale Supérieure des Mines de Saint-Etienne, Laboratoire de Céramiques Spéciales, CNRS URA 1884,158 Cours Fauriel, F-42023 Saint-Etienne cedex 02, France ;

³Centre d'Etudes de Cadarache, CEA/DEN/CAD/DEC/SPUA/LMPC, Bât. 717,F-13108 Saint Paul lez Durance cedex

Abstract

UO₂ powder containing 5% of almost spherical defects of controlled size have been sintered. The defects were prepared with the same powder by presintering either the natural powder aggregates or partially milled pressed powder. Systematic image analysis was performed to get the local microstructure features inside the defects and in the matrix outside the defects. The set of results is used here as a sintering database with three identified sintering “constraint” parameters (compaction level C_0 , radial distance r to the defect edge, and sintering “history” H) and three microstructure “responses” (pore volume fraction V_V^P , pore mean diameter D_P , and grain mean diameter D_G). Data analysis in the 3D responses space shows that these variables are not independent but define a unique surface, on which each point corresponds to a set of constraints (C_0, r, H).

1. 1. Introduction

Heterogeneities are always present in green compacts and evolve during sintering [1,2,3]. These heterogeneities, such as aggregates or large pores, are the source of microstructural defects which exert a serious and detrimental influence on mechanical and thermo-mechanical properties of the material. The effects of these heterogeneities have been observed and in some cases interpreted [4,5,6], but most of the quantifications are macroscopic: experimental laws of local microstructures evolution that should enable to validate computer simulations of sintering with heterogeneities are still lacking. The present paper is issued from a study which aims to bring out a better understanding of the effects of different heterogeneities on the sintering of their surrounding microstructure by means of a quantitative analysis of different microstructural characteristics [7]. The results mainly rely on local microstructural information obtained by quantitative image analysis for a set of experiments with controlled defects and chosen sintering conditions on a spray dried uranium dioxide powder. The obtained data are here analysed from a statistical point of view.

2. 2. Experimentals

2.1. Defects

The defects were obtained from the same UO₂ powder, in order to avoid any uncontrolled chemical effect of the defects. Two types of defects have been used (Fig.1):

- simple natural aggregates, without any compression,
- compact aggregates obtained from powders compressed at 200MPa, followed by a ball milling of the compacts.

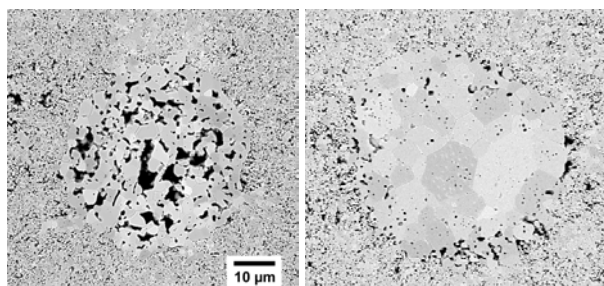


Fig .1. Cross section of samples sintered at 1500°C, containing two types of defects : a) simple aggregate ($C=0$); b) compact aggregate ($C=1$). Both of them have been consolidated at 1700°C.

Both kinds of aggregates were calibrated in the range 40-60 μm by sieving, then sintered in different conditions to get 3 levels of consolidations (Fig. 2). 6 different kinds of defects were therefore obtained, corresponding to two compaction conditions (denoted by $C=0$ and $C=1$ for natural aggregates and 200MPa compacted aggregates respectively), and 3 consolidation cycles (Fig. 2): 1600°C, 1700°C 15min and 1700°C 120min.

2.2. Sintering experiments

Green compacts containing a low rate (3 vol%) of a specific kind of aggregates were prepared and sintered at different temperatures (Fig 2): 1500°C, 1600°C, 1700°C, 1700°C 20min or 1700°C 60min.

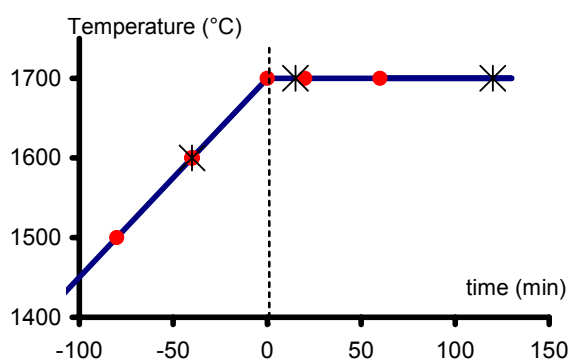


Fig. 2. Temperature cycles used for the consolidation of aggregates (stars) and sintering experiments (disks). The heating rate up to the plateau is 150°C per hour.

2.3. Local microstructure analysis

Etched polished sections of the samples were investigated in the vicinity of likely isolated heterogeneities. A fine mapping of the heterogeneity and its surrounding matrix, obtained by Field Emission Scanning Electron Microscopy, was processed by image analysis. The measured area, centered on the heterogeneity, is about 150 x 150 μm^2 .

Systematic measurements were performed, in order to get the local microstructural characteristics as functions of distance to the defect edges. This was obtained by defining isodistance regions using image analysis classical tools (Fig. 3). These regions, referred with the corresponding distance r , are therefore used as masks to get average values of microstructure parameters.

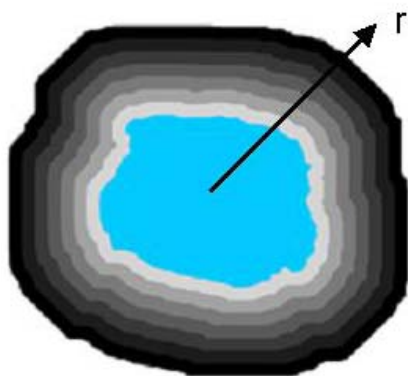


Fig. 3. Starting from a hand drawn contour of a defect, isodistance regions are obtained using classic mathematical morphology operators [8,9], dilatations for outside distances ($r > 0$), erosions for inside distances ($r < 0$).

Among the numerous possible microstructural characteristics [10,11], three will be discussed here:

- the pore volume fraction V_V^P ("porosity"), measured from the 2D area fraction on images
- the grain diameter D_G , measured from the (2D) area of each grain section (diameter of the circle with the same area)
- the pore diameter D_P (*idem*)

Mean values are calculated using in each isodistance region ; for diameters, area weighed average values are

used, so that each grain (resp. pore) accounts for the part of it which is in the considered region.

3. Analysis of results

3.1. Local analysis

The results have first been analysed [7] on the basis of the evolution of profiles to get information on the local evolution during sintering. For instance, in the case of medium consolidated compact aggregates (1600°C) (Fig. 4), the influence of distance r from the defect edge is limited to a relatively short range, smaller than the defect radius, while a strong influence ("constrained sintering"?) is observed inside the defect.

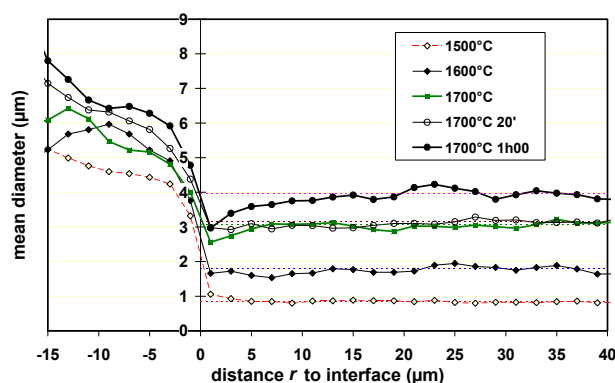


Fig. 4. Evolution of the mean grain diameter as a function of distance r to the defect-matrix interface, for different sintering temperatures, in the case of compact aggregates consolidated at 1600°C. Dotted lines indicate the mean value in the matrix.

This kind of analysis leads to detailed useful results, either on each kind of samples, or by comparing the different samples and defects with each other.

3.2. Statistical analysis

A different analysis has been tried in the present paper. Considering the set of data obtained on each point (each region) as a whole, we have searched for possible common features, which could be representative of the sintering processes involved in the sintering of this ceramic.

In this purpose, we consider that the measured microstructure parameters (pore volume fraction V_V^P , pore mean diameter D_P , and grain mean diameter D_G) are characteristic "responses", through the sintering mechanisms, to three identified sintering "constraint" parameters : the compaction level C , the radial distance r to the defect edge, and sintering "history" H .

The sintering "history" is the result of the sintering cycle of a given point of a given sample. It must be noticed that, while points located in the matrix regions have a single sintering cycle, points located in the defects have a double sintering, constituted by the "consolidation" and the "sintering" cycles. A simple practical semi-quantitative classification of the points "history" is used here, by way of a scale H defined by :

$$H = H_0 + 0.01 t$$

where is H_0 is an integer value which is associated to the higher temperature at which the considered point has been sintered (0, 1, 2 for $T= 1500, 1600, 1700$ respectively), and t the total duration of the plateau(s) at this temperature. This leads to a very “easy to read” parameter : $H = 2.6$ simply means that the considered region has been sintered at the maximum temperature $T= 1600$ for 60 minutes. Of course this classification would be ambiguous if experiments at 1500 or 1600°C for more than 100 minutes had been performed... which is not the case.

The first step was to search for direct correlations through scattering diagram between pairs of parameters (Figs. 5 and 6). Fig. 5 clearly evidences no correlation between pores and grains diameters. An influence of the sintering history H can be seen on Fig. 6 when this parameter is visualised (the expected pore volume decrease during sintering), no correlation appears on other scattering plots.

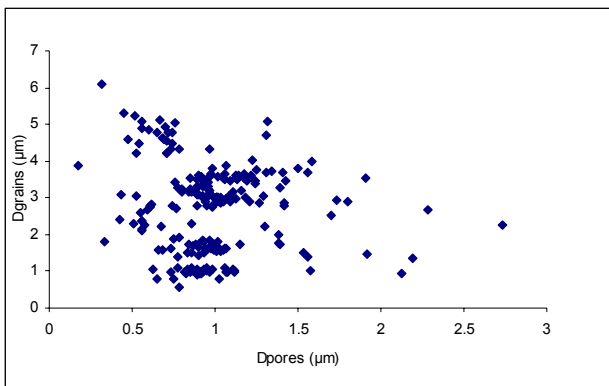


Fig.5 : Scattering diagram between grain diameters (D_G) and pore diameters (D_P) for a subset of data (samples at different temperatures with compact aggregates consolidated at 1500°C)..

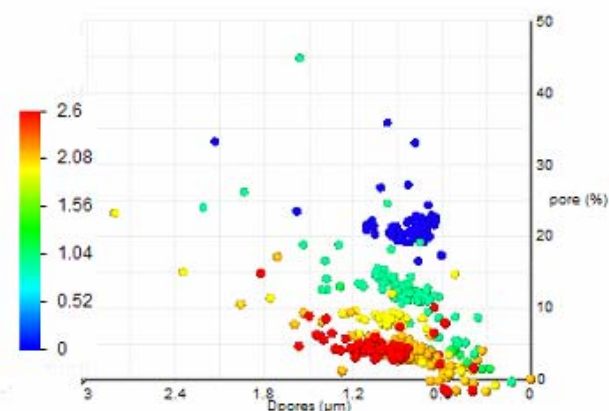


Fig.6. Scattering diagram between pairs pore diameter and pore volume fraction (%) on a subset of data of compacted aggregates and matrix ($C= 1$). The color scale indicates the sintering history parameter H .

But more interesting observations can be obtained from plots in the 3D responses space (V_V^P, D_P, D_G), as shown on Figs. 7 and 8.

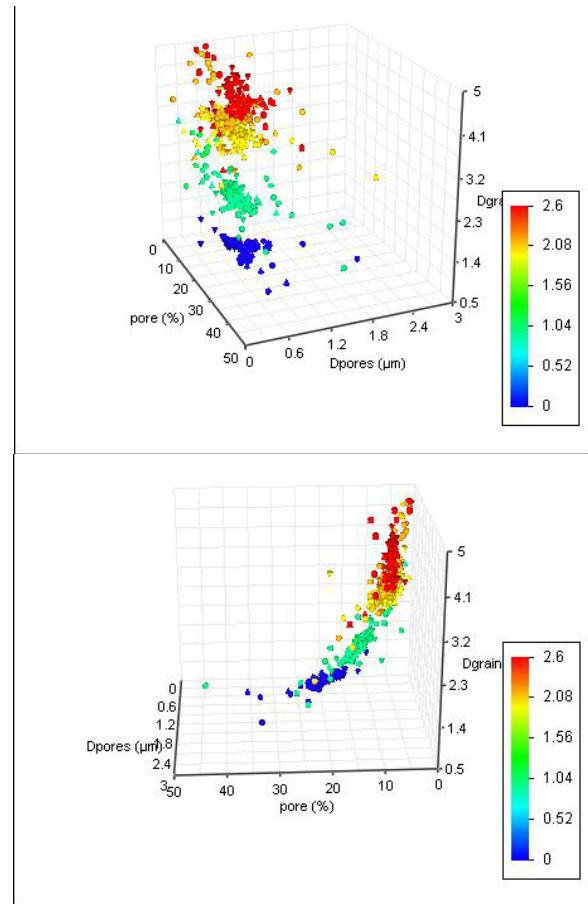


Fig. 7. Plots of data in the 3D responses space (V_V^P, D_G, D_P), seen from two different angles, for a subset of data of compacted aggregates and matrix ($C_0= 1$). The second view clearly evidences that all points are located around a 2D surface in the 3D space. Points on this surface are placed according to the sintering history.

The plots of Fig.7 show that the characteristic experimental points from different samples are located in the vicinity of a unique 2D surface in the 3D space. This means that the 3 parameters are not independent and have correlated evolutions during sintering. Each point on this surface corresponds to a set of constraints (C, r, H). The color code associated with the sintering history parameter H indicates the direction of time evolution. Sintering trajectories can be expected to be perpendicular to the iso- H curves on the surface, but further analysis must be performed to check this hypothesis.

Fig. 7 corresponds to regions (points) with 200MPa compaction ($C=1$) ; points corresponding to natural aggregates ($C=0$) are placed on an other part of the 2D surface, corresponding to larger pore diameters and pore fraction (Fig. 8).

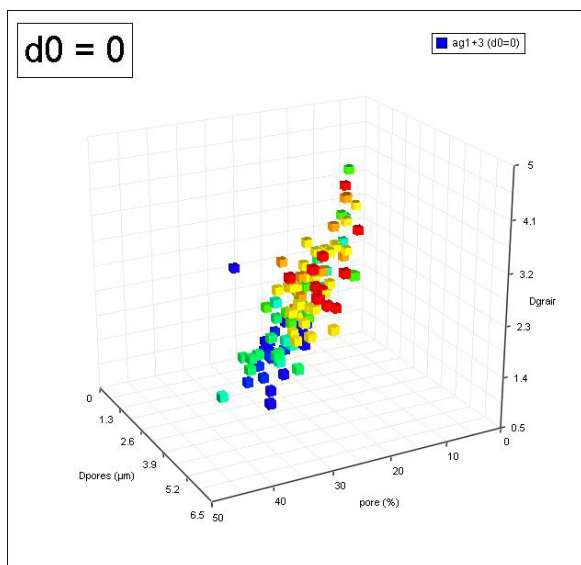
4. Conclusions

The analysis presented in this paper was made possible by the availability of a large set of data obtained by local image analysis on samples with controlled defects. It is clear that the approach is not limited to such cases, but only needs a set of microstructural data corresponding to different values of sintering constraints, *i.e.*, the possibility to make some statistical analysis of results.

Although only one powder was used in this work, we can expect that the correlations evidenced in this paper through 3D plots between grain diameter, pore diameter and pore fraction indicate that the evolutions of these microstructure characteristics are strongly correlated. Further analysis is also needed to explore more accurately the influence of the different sintering constraints (C_0, r, H).

At this point, this can only be considered as an empirical observation, and modelling of mechanisms should be needed to explain this correlation.

However, practical use of these results can already been made: first as a knowledge of which regions in the 3D space, *i.e.*, which kinds of microstructures can be reached or not by sintering ; second, as a guide to choose the sintering conditions.



Fig

Fig. 8 Plots of data in the 3D responses space (V_V^P, D_G, D_P), for a subset of data of natural aggregates ($C_0=0$).

5. References

- [1]. F.F. Lange, Sinterability of agglomerated powders, *J. Am. Ceram. Soc.* 67(2), 83-89 (1984)
- [2]. L.C. Lim, P.M. Wong and M. Jan, Microstructural evolution during sintering of near-monosized agglomerate-free submicron Alumina powder compacts, *Acta Materialia*, 2263-2275 (2000)
- [3]. M. Ciftcioglu, M. Akinc, L. Burkhart, Effect of agglomerate strength on sintered density for Ytria powders containing agglomerates of monosize spheres, *J. Am. Ceram. Soc.* 70 (11), p.C-329-C334, 1987.
- [4]. K. Uematsu Y. Zhang, N. Uchida, Characteristics and formation mechanisms of defects in Alumina powder compacts", *Ceram. Trans.* 51, p.263-270, 1995.
- [5]. N. Shinohara , M. Okumiya, T. Hotta, K. Nakahira, M. Naito, K. Uematsu, Morphological changes in process-related large pores of granular compacted and sintered Alumina *J. Am. Ceram. Soc.* Vol. 83, n°7 (2000), p. 1633-40.
- [6]. A.G. Evans, Considerations of inhomogeneity effects in sintering, *J. Am. Ceram. Soc.* Vol. 65, n°11 (1982), p. 497-501.

[7]. E.Girard, F.Valdivieso, P.Goeuriot, JM.Chaix, J.Léchelle, G.Chiarelli *Key Engineering materials* 264-268, 197-200 (2004)

[8]. J.Serra, *Image analysis and mathematical morphology*, Academic Press, 1982

[9]. L. Wojnar, *Image analysis : Applications in material engineering*, CRC Press, 1999

[10]. R.T. De Hoff, F.N. Rhines, *Quantitative Microscopy*, McGraw Hill, New-York, 1968

[11]. J.M.Chaix, *Image analysis, microstructure evolution and sintering mechanisms*, STERMAT 2000 - VI International Conference on Stereology and Image Analysis in Materials Science., Krakow, Poland, 20-23 September 2000